

Rapid Detection and One-Step Differentiation of Cross-Reactivity Between Zika and Dengue Virus Using Functional Magnetic Nanosensors

Tuhina Banerjee, Truptiben Patel, Oleksandra Pashchenko, Rebekah Elliott, and Santimukul Santra*

Cite This: *ACS Appl. Bio Mater.* 2021, 4, 3786–3795

Read Online

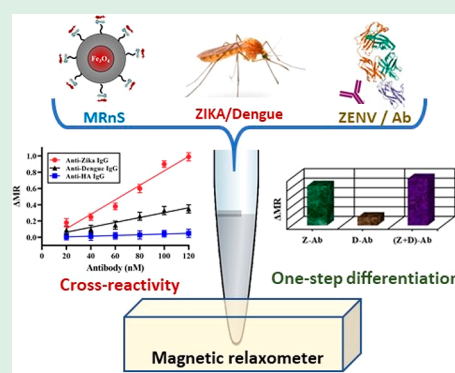
ACCESS |

Metrics & More

Article Recommendations

ABSTRACT: Infection with the Zika virus (ZIKV) is an ongoing problem especially as accurate, cost-effective testing remains unresolved. In addition, coinfection occurs with both the Dengue virus (DENV) and ZIKV which leads to cross-reactivity between the flaviviruses and can result in false positives and inaccurate testing. This supports the current need for a simple assay that can detect Zika antibodies sensitively that at the same time can differentiate between cross-reactive antibodies. In this study, we developed customizable magnetic relaxation nanosensors (MRnS) conjugated to various ligands, which included ZIKV (ZENV, zika domain III and NS1) and DENV proteins for specific detection of cross-reactive Zika and Dengue antibodies. Binding interactions between functional MRnS and corresponding targets resulted in the change in spin–spin magnetic relaxation time (T2MR) of water protons, allowing for a rapid and simple means by which these interactions were detected and quantified. Our results show the detection of Zika antibodies within minutes at concentrations as low as 20 nM and display high specificity, reproducibility, and analytical sensitivity. Furthermore, a mixture of functional MRnS was used for the one-step simultaneous detection and differentiation of Zika and Dengue infections. These results demonstrate high specificity and sensitivity for the detection of ZIKV and DENV despite coinfections in both simple and complex media. Overall, our magnetic nanoplatform could be used as a rapid and sensitive assay for the detection of not only Zika- and Dengue-related testing but can be further applied to serological samples of any other pathogens.

KEYWORDS: nanosensor, zika detection, dengue virus, cross-reactivity, magnetic relaxation



INTRODUCTION

The Zika virus (ZIKV), an arthropod-borne virus in the Flaviviridae family, first emerged as a potential health risk in 2007, on Yap Island.¹ Rising from relative obscurity in comparison to other flaviviruses such as Dengue (DENV), West Nile virus (WNV), and Yellow Fever virus (YFV), ZIKV spread to the Americas with the first confirmed case in Brazil in May, 2015,² and quickly surged to 170 000 confirmed cases by 2016.³ This rapid geographical expansion, coupled with an increase in neurological disorders in both unborn children and adults, led the World Health Organization (WHO) to declare the flavivirus a public health emergency of international concern (PHEIC) in 2016. By 2017, 84 countries had been infected, including the United States.⁴ Complications of ZIKV infection have continued to emerge. A causal relationship was established with Guillain–Barré syndrome (GBS) in adults. Often asymptomatic, ZIKV is of particular concern as it is also now known to be sexually transmitted and can result in congenital Zika syndrome (CZS),^{5,6} causing central nervous system malformations in developing fetuses including fatal encephalitis and other congenital defects such as lissencephaly, ventriculomegaly, and ocular abnormalities.^{7–10} Therapeutic

interventions are vital to protect against ZIKV and potentially severe consequences. However, molecular mechanisms for viral infectivity are still not fully understood and hinder robust methods for rapid, accurate ZIKV testing. Antibody testing, for example, can be affected by cross-reactivity obscuring results, particularly when patients have been previously affected by DENV.¹¹ Knowing which flavivirus is the infective agent and understanding pathogenic mechanisms are crucial for treatment and intervention.

However, rapid and accurate diagnostic testing remains problematic as the WHO ASSURED criteria that requires tests be affordable, sensitive, specific, user-friendly, rapid and robust, equipment-free, and deliverable remains elusive.^{12,13} Cross reactivity is of particular concern as distinguishing between the

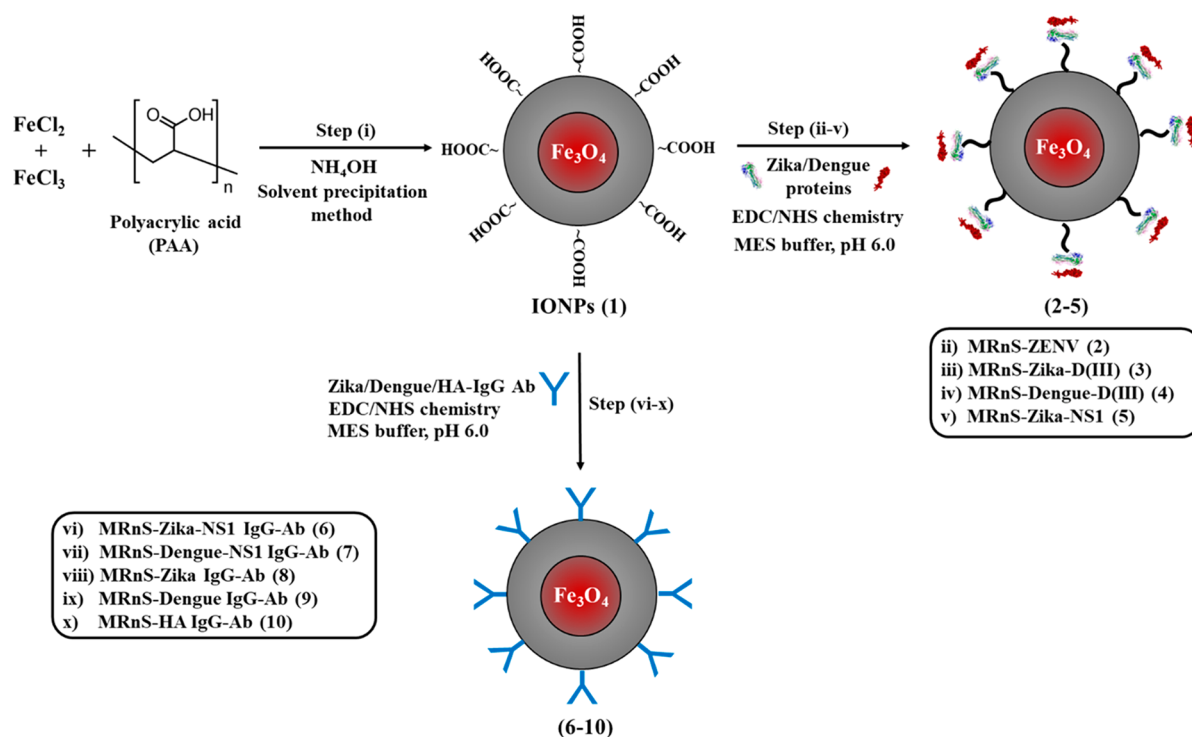
Special Issue: Functional Biomaterials for Infectious Diseases

Received: September 29, 2020

Accepted: December 17, 2020

Published: December 30, 2020



Scheme 1. Synthesis of Functional MRnS^a

^aIron oxide nanoparticles (1, IONPs) were synthesized using solvent precipitation method. Functionalization of IONPs with Zika and Dengue proteins (2–5) and antibodies (6–10) using EDC/NHS chemistry to formulate functional MRnS.

two arboviruses is essential for detection and patient care with widespread infection of ZIKV in recent years and DENV being present in 128 countries, placing an estimated 3.9 billion people at risk of infection.^{14,15} As of 2018, five serological and 14 molecular assays were commercially available with the United States Food and Drug Administration (FDA) under emergency use authorization (EUA).¹⁶ Despite these assay options, limited resources hinder clinical diagnoses in many countries where ZIKV is endemic.¹⁷ Resource paucity requires tests be sent internationally for processing, delaying results, and increasing burdens. Additionally, sensitivity, specificity, as well as cross-reactivity hinder accurate testing. For example, RNA detection is the most sensitive during the first week of ZIKV only with various serological tests such as real-time PCR (RT-PCR) tests, but they have persisted as frontline molecular assays.^{17,18} Antibody (Ab) tests, such as IgM assays, which include ELISA, are more sensitive for later testing as IgM increases from around day 4 from symptom onset,^{19–21} peaks at 11 days, and decreases by 20 days postinfection.²² Further complicating optimal assays is the high cross-reactivity in secondary flavivirus infections observed, especially in DENV and ZIKV.^{19,23,24} Endemic Dengue transmission in settings confounds testing with more current assays such as ZIKV IgM-ELISA demonstrating high specificity but poor sensitivity.²⁵ Testing remains complicated due to timing, accuracy, and cost. Furthermore, some assays such as the plaque reduction neutralizing test (PRNT), which addresses specificity and has been used as a confirmatory test since the 1950s, require laborious methods making them not feasible for large-scale surveillance.²⁶

Rapid diagnosis is vital for viral containment through clinical treatment and successful monitoring and protection of public health.^{27,28} Nanobiotechnology is a rapidly advancing field that

is emerging with new developments with numerous benefits including biosensors for rapid detection and diagnosis of mosquito-transmitted viral infections.^{29–31} To reduce cross-reactivity between ZIKV and DENV, Zhang et al. developed a plasmonic-gold multiplexed assay measuring IgG and IgA antibodies instead of IgM to reduce cross-reactivity with DENV.³² Yen et al.'s study demonstrated that multicolored silver nanoplates could be used to differentiate among bioreceptors and utilized this multiplexed pathogen detection for DENV and YFV.³³ Sensitivity and selectivity have been enhanced through improvements with lab-on-a-chip devices and nanoparticles changing colors when aggregated. Limitations previously observed with biosensors designed to detect nonstructural (NS) type proteins, produced from day 5 of infection, have been overcome by basing an optical sensor on the surface plasmon resonance phenomenon.^{34,35} Earlier diagnosis of DENV was possible through detection of DENV structural E-protein which forms the host virus coat.³⁵ Biosensors are able to quickly recognize analytes despite complex matrices or low concentrations without pretreatment requirements, lengthy sample preparation, or lengthy sample treatments. This is possible due to the ability of biosensors to produce quantifiable electric signals from biologically selective responses.³⁶ Improvements in biosensing technology is paving a way for real-time diagnoses that are accurate, rapid, cost-effective, and easy to use, especially important in ZIKV and other flavivirus infections, with more work still to be done.

In this work, we focused on magnetic relaxation technique to detect ligand interactions using functional iron oxide nanoparticles (IONPs). Biomolecular targets, such as ZIKV antibodies (Abs) and proteins, bind to the IONP surface replacing the surrounding water, which results in measurable changes in the solution's spin-spin magnetic relaxation times

($\Delta T2MR$). Targeting proteins with high specificity for ZIKV and utilizing magnetic resonance (MR) imaging, we have conjugated specific proteins and antibodies, interchangeably, with our magnetic resonance nanosensor (MRnS). By doing so, we were able to test sensitivity and specificity in the presence of DENV Abs and proteins and immunological cross-reactivity between these two antigenically and structurally highly similar flaviviruses. Our studies indicate Abs from the ZIKV NS 1 (Z-NS1) region and ZIKV domain III (Z-D-III) are more specific for ZIKV, with NS1 indicating higher specificity, and contribute to gathering evidence these Abs could be utilized for accurate assays even when DENV coinfection is present. Furthermore, our functionalized MRnS platform can be utilized for fast, cost-effective, and convenient assays that would satisfy WHO ASSURED criteria for accurate point-of-care testing globally and, especially, as indicated for resource-challenged areas.

MATERIALS AND METHODS

Chemicals. Iron salts, ferric chloride ($\text{FeCl}_3 \cdot 6\text{H}_2\text{O}$) and ferrous chloride ($\text{FeCl}_2 \cdot 4\text{H}_2\text{O}$), hydrochloric acid, and ammonium hydroxide were obtained from Fisher Scientific (ACS grade). Polyacrylic acid (PAA), 2-morpholinoethanesulfonic acid (MES), and *N*-hydroxysuccinimide (NHS) were purchased from Sigma-Aldrich. 1-Ethyl-3-[3-(dimethylaminopropyl) carbodiimide hydrochloride (EDC) was obtained from Pierce Biotechnology. Dialysis bags with molecular weight cutoff 6–8 kDa were obtained from Spectrum Chemicals. Zika envelope protein (ZENV) and the corresponding Anti-ZENV Ab were obtained from Alpha Diagnostics. Zika reporter virus particles (RVPs) were kindly gifted by Integral Molecular for research. Other proteins including Zika envelope domain III (Z-D-III), Dengue envelope domain III (D-D-III), Z-NS1, Dengue NS1 (D-NS1), and the other paired NS1 antibodies were obtained from ProSpec Bio. Z-D-III Ab was purchased from Absolute Antibody. Hemagglutinin (HA) and the Anti-HA IgG were acquired from Sino Biological.

Synthesis of Iron Oxide Nanoparticles (1, IONPs). IONPs were synthesized using our previously reported protocol,^{37–39} as shown in Scheme 1. Briefly, three solutions were prepared: solution 1 containing 0.62 g of FeCl_3 , 0.35 g of FeCl_2 , and 2 mL of water. Solution 2 contained NH_4OH (1.8 mL of 30% stock). Solution 3 was prepared by dissolving 0.86 g PAA in 5 mL of water. Once these solutions were prepared, initially 90.0 μL of 12 M HCl was added to solution 1, followed by the addition of solution 2 with continuous vortexing at 875 rpm. Solution 3 was added to the resulting mixture and the reaction mixture was allowed to incubate at room temperature for an hour. The resulting solution was centrifuged for 30 min at 4000 rpm to precipitate the agglomerates and larger nanoparticles. The supernatant was then dialyzed (dialysis bags with MWCO 6–8 kDa) in PBS pH = 7.4, and the final concentration of the purified IONPs was adjusted to $[\text{Fe}] = 4.0$ mM by adding PBS (1X, pH 7.4) and a baseline T2MR was recorded. For repeatability of the synthetic protocol, three separate IONPs preparations were made using the same protocol, followed by the measurement of size, zeta, and T2MR values.

Conjugation of Proteins and Antibodies on the Surface of IONPs (2–10). To formulate functional MRnS, freshly prepared IONPs (5 mL; 4.0 mM) were diluted with 5.0 mL of PBS (1X, pH 7.4). Then, EDC (8 mg in 250 μL MES buffer, pH 6.0) was added to the IONPs solution, followed by the addition of NHS (5 mg in 250 μL MES buffer, pH 6.0) in small increments at room temperature with slow mixing. After 3 min, a targeting ligand solution was added dropwise containing selected proteins and antibodies (10 μL , 1.0 mM). The reaction mixture was kept on a table-top mixer for 2 h and then transferred to 4 °C overnight. The solution was then purified via a magnetic column to separate unconjugated antibodies, proteins, and other free reagents. Particle size, zeta potential, and T2MR of the functional MRnS was compared with that of carboxylated IONPs (1) for successful conjugation. Change in T2MR before and after

conjugations was used for the assessment of reproducibility parameter. Concentration of functional MRnS was adjusted to $[\text{Fe}] = 2.0$ mM and a baseline T2MR value was set in the range of 120 ms (ms).

Characterizations. Conjugated IONPs were purified using a QuadroMACS magnetic LS column from Miltenyi Biotec. For the overall size and zeta potential measurements of MRnS, Malvern's zetasizer NANO-ZS90 was used. TEM experiments were performed using JEOL JEM-2100 instrument. A bench-top magnetic relaxometer from Bruker (mq20, 0.47 T) was used for the collection of spin–spin magnetic relaxation time designated as T2MR. Surface plasmon resonance (SPR) experiments were performed on a Reichert's dual-channel SR7500 DC SPR system.

Measurement of Spin–Spin Magnetic Relaxation Time for MRnS Binding Assays. To conduct the binding assay, different solutions of proteins and antibodies with varying concentrations (10–120 nM) were prepared. To each of these solutions, a fixed amount of MRnS ($[\text{Fe}] = 2.0$ mM) was added and then incubated for 30 min at 25 °C. After 30 min, T2MR values were measured. For each of these sample solutions, a control containing the MRnS without any proteins or antibodies was prepared and run in parallel. T2MR values obtained from the control samples were subtracted from each experimental value in order to obtain effective ΔMR of binding. For each measurement, T2MR data was collected in triplicate. The data was normalized for comparative analysis using the following equation:

$$\Delta\text{MR} = \frac{\Delta T2}{\Delta T2_{\text{max}}}$$

In our MR assay, $\Delta\text{MR} \geq 0.1$ was considered positive interaction and $\Delta\text{MR} \leq 0.1$ was considered as minimal or no binding. Similar protocol was used when T2MR readings were collected in complex media such as plasma. For assessment of reproducible parameter, three independent preparations of antizika IgG conjugating MRnS ($[\text{Fe}] = 2.0$ mM), and the batch to batch variability in detection sensitivity was evaluated using samples of ZENV, Z-RVP, Z-D(III), DENV, and HA (each at 120 nM and spiked in 1X PBS).

For time-dependent experiments, three experimental solutions were prepared: ZENV (50 nM) was mixed with antizika/antidengue/anti-HA-MRnS ($[\text{Fe}] = 2.0$ mM) and T2MR readings were collected throughout a 60 min period. The first experimental data point was collected after 3 min of mixing. For one-step detection between Zika and Dengue, a combination of MRnS mixture featuring 80 μL of MRnS-Zika-D(III) ($[\text{Fe}] = 2.0$ mM) and 20 μL of MRnS-Dengue-D(III) ($[\text{Fe}] = 2.0$ mM) was incubated with anti-Zika IgG (100 nM) or anti-Dengue (100 nM), or a combination of both the Abs (100 nM each). T2MR readings were recorded after a 30 min incubation for each of these test solutions containing Abs.

Surface Plasmon Resonance Experiments (SPR). SPR experiments were performed on Reichert SR7500DC at 25 °C. Zika full-length envelope protein ZENV and Zika-D(III) were immobilized on a CMS sensor chip. Activation of the sensor chip was achieved by injecting a mixture of 40 mg/mL of EDC and 10 mg/mL of NHS. After activation, a 10 min injection of 1.0 mol/L ethanolamine (pH 8.5) was used to block the unreacted sites on the sensor chip. ZENV was immobilized on the sensor chip around 1500 μRIU . Anti-Zika-IgG (120 nM), anti-Dengue-IgG (120 nM), and anti-HA-IgG (120 nM) were perfused as a ligand over the ZENV at a flow rate of 50 $\mu\text{L}/\text{min}$. After each cycle, the sensor surface was regenerated with a short injection of 10 mM NaOH at a rate of 50 $\mu\text{L}/\text{min}$ for 15 s. Antibodies were diluted in 1X PBST containing 3.0 mM EDTA.

Data Analysis. Plots were created and the analysis of the data was performed using GraphPad Prism 7 (Graphpad Software Inc.). The average of three independent experiments is described, and all experimental values are reported as mean \pm standard error of the mean. Unpaired *t* tests were performed for T2MR measurements. $P < 0.0001$ or **** was considered statistically significant.

RESULTS AND DISCUSSION

Synthesis and Characterization of MRnS. In this study, we propose a functionalized MRnS for the rapid detection of

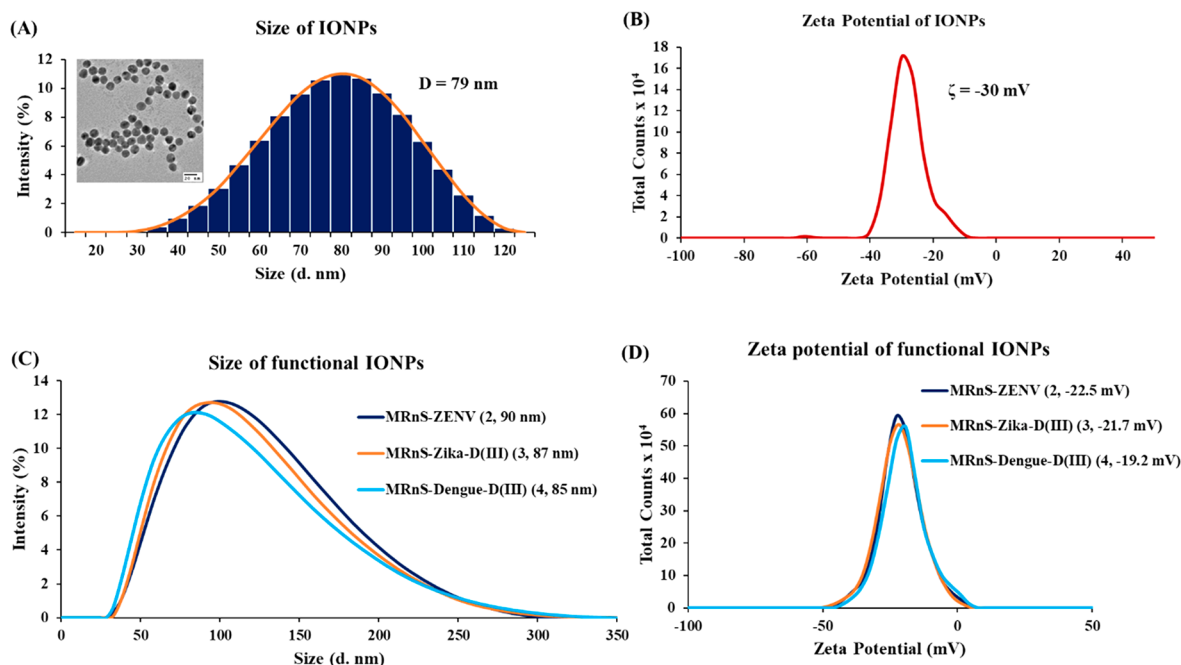


Figure 1. Characterization of IONPs and Zika/Dengue proteins conjugated MRNs. Average hydrodynamic diameter measurement using dynamic light scattering (DLS) of (A) IONPs (1) 79 nm. (inset) TEM image showing the Fe_3O_4 core size of 10 nm (scale bar: 20 nm). (C) MRnS-ZENV (2) 90 nm, MRnS-Zika-D(III) (3) 87 nm, and MRnS-Dengue-D(III) (4) 85 nm. Measurement of zeta potentials (B) before and (D) after conjugation.

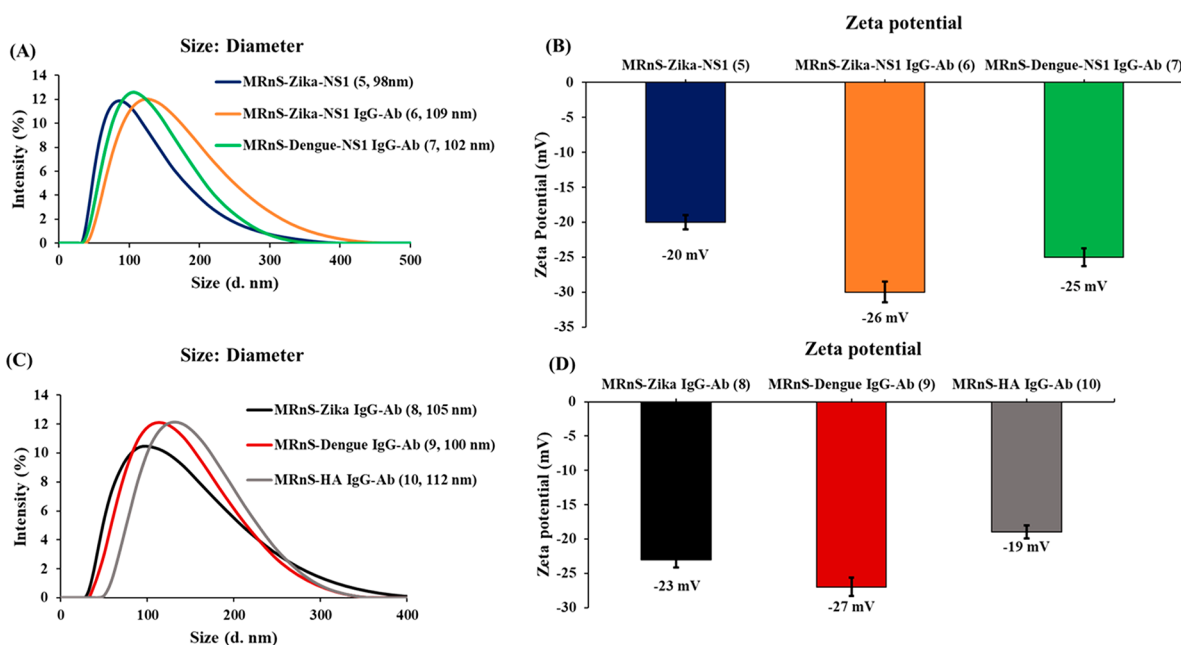


Figure 2. Determination of hydrodynamic diameter by DLS of various functional MRNs (A and C): MRnS-Zika-NS1 (5) 98 nm, MRnS-Zika-NS1 IgG-Ab (6) 109 nm, MRnS-Dengue-NS1 IgG-Ab (7) 102 nm, MRnS-Zika IgG-Ab (8) 105 nm, MRnS-Dengue IgG-Ab (9) 100 nm, and MRnS-HA IgG-Ab (10) 112 nm. (B and D) As shown, zeta potentials of corresponding functional MRNs (5–10) were measured using DLS.

ZIKV infection endemic to areas with populations previously or simultaneously infected with DENV. We hypothesized that our MRnS platform would reduce false positives by increasing specificity and allow for interchangeable methods resulting in a customizable MRnS for patient care needs in different regions. Furthermore, we wanted to assess findings of cross-reactivity antibody responses between ZIKV and DENV in serological testing. To do so, we first synthesized IONPs using our previously reported synthetic protocol⁴⁰ and detailed in

Scheme 1. Briefly, iron salts and PAA polymer solutions were prepared and mixed with NH_4OH solution in a stepwise fashion and the final concentration of synthesized IONPs (1) was adjusted to $[\text{Fe}] = 4.0$ mM. By using EDC/NHS chemistry, IONP's surface carboxylic acid groups were functionalized with the targeting antibodies/proteins. This bioconjugation is a critical step for the formulation of various functional MRnS (2–9), which allows for the specific binding when a target solution is added. Influenza antibody (anti-HA

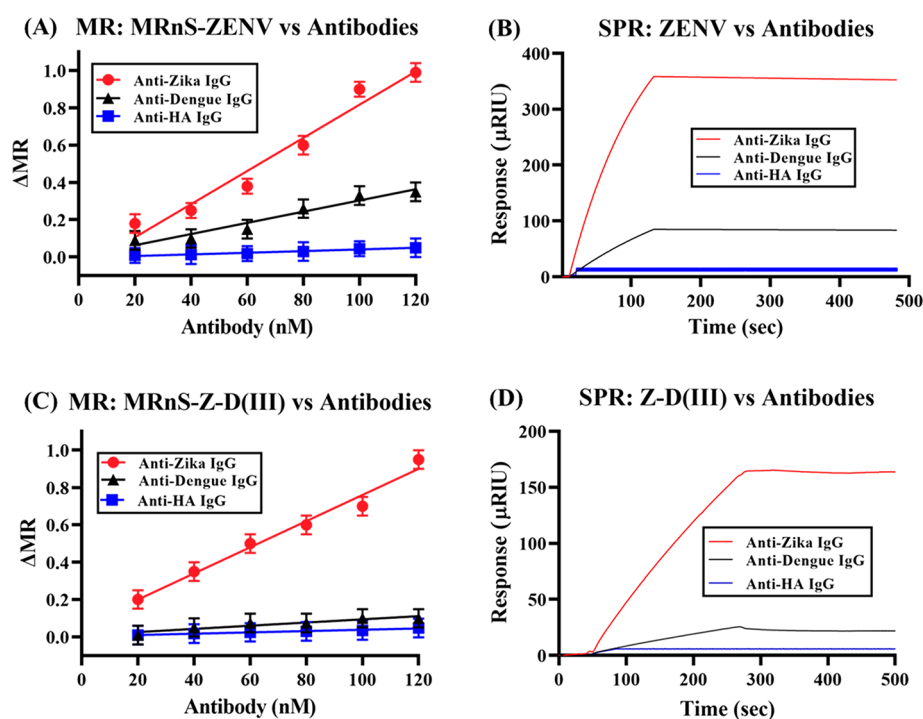


Figure 3. Measurement of cross-reactivity and detection specificity by magnetic relaxation and surface plasmon resonance assays. (A and C) MRnS-ZENV/MRnS-Z-D(III) ($[\text{Fe}] = 2.0 \text{ mM}$) was incubated with increasing concentrations (10–120 nM) of anti-Zika IgG and anti-Dengue IgG for 30 min at 25 °C. Anti-HA IgG was selected as a control. Error bars are reported as mean \pm standard error of the mean. (B and D) SPR traces showing direct interaction between ZENV/Z-D(III) and corresponding antibodies. ZENV/Z-D(III) was immobilized around 1500 μRIU and anti-Zika-IgG/anti-Dengue-IgG (each at 120 nM) was perfused over the Zika proteins. Anti-HA IgG was chosen as control. Results are representative of two independent experiments.

IgG Ab) conjugated MRnS (10) was synthesized to be used as negative control for the Zika/dengue binding experiments. We first used dynamic light scattering (DLS) measurements to evaluate hydrodynamic diameter, zeta potential and overall stability of our PAA polymer-coated IONPs (1). The average size was found to be $79 \pm 2 \text{ nm}$ with a negative surface charge of -30 mV , respectively (Figure 1A and 1B). Transmission electron microscope (TEM) experiments showed the formation of an iron oxide core of 10 nm. Next, we performed experiments for successful conjugation by comparing size and zeta potential of our functional MRnS. Conjugated IONPs showed various size distributions in the range of 85 to 112 nm (Figures 1C and 2A and C) and negative surface charge with ranges from -19 to -27 mV (Figures 1D and 2B and D). These results further indicate the successful conjugation as there was an increase in hydrodynamic radius and statistically significant change in zeta potential value after each conjugation with different proteins and antibodies.

Functionalized MRnS for Specific ZIKV Detection. By testing each of our functional MRnS, we were able to demonstrate levels of specificity and cross-reactivity utilizing a T2MR diagnostic technique. We hypothesized that binding of functional MRnS to the corresponding target protein or antibody results in the displacement of water molecules around the MRnS and leads to measurable changes in the spin–spin magnetic relaxation time ($\Delta\text{T}2\text{MR}$). Furthermore, as the concentration of the target antibodies/proteins increase, the linear trend in $\Delta\text{T}2\text{MR}$ values is expected if effective binding occurs with the MRnS. In our studies, solutions of anti-Zika IgG/anti-Dengue IgG antibody were prepared in increasing concentrations from 10 to 120 nM. A fixed amount of

functional MRnS at $[\text{Fe}] = 2.0 \text{ mM}$ was then added to each. A baseline T2MR measurement was taken after 30 min of incubation without using any target. The T2MR data was then normalized using the equation outlined in the experimental section and expressed in ΔMR . Considering the extensive cross-reactivity that may exist between Zika and Dengue envelope proteins, we began our studies by examining the interaction of MRnS-ZENV (2) and anti-Zika IgG/anti-Dengue IgG (Figure 3A). As the concentration of Zika antibody increases, so too does the binding with MRnS-ZENV as reflected by increase in the ΔMR value. Although anti-Zika IgG exhibited highest binding affinity, it is important to note that dengue IgG also bound to some extent with MRnS-ZENV (ΔMR of 0.9 and 0.3 for Zika and Dengue IgG, respectively). Moreover, in our experiments, we were able to detect these antibodies at concentrations as low as 20 nM within minutes. In contrast, no binding was observed in the presence of anti-HA IgG (negative control with ΔMR 0.01). This further confirms the capability and potential application of our functional MRnS for identifying cross-reactivity between Zika and Dengue infections in a precise manner. After we verified the usefulness of our MRnS for detecting cross-reactivity, we wanted to investigate whether specific detection of Zika could be achieved. In this context, Zika domain III conjugating IONPs, MRnS-Z-D(III) 3 was formulated and mixed with different amounts of Zika and Dengue antibodies, respectively. As shown from recent studies,²² D(III) of ZIKV shares only 29% amino acid identity with D(III) DENV and therefore is expected to facilitate in their detection and differentiation. The magnetic relaxation results are shown in Figure 3C. Anti-Zika IgG showed maximum binding interaction with ΔMR of 0.9.

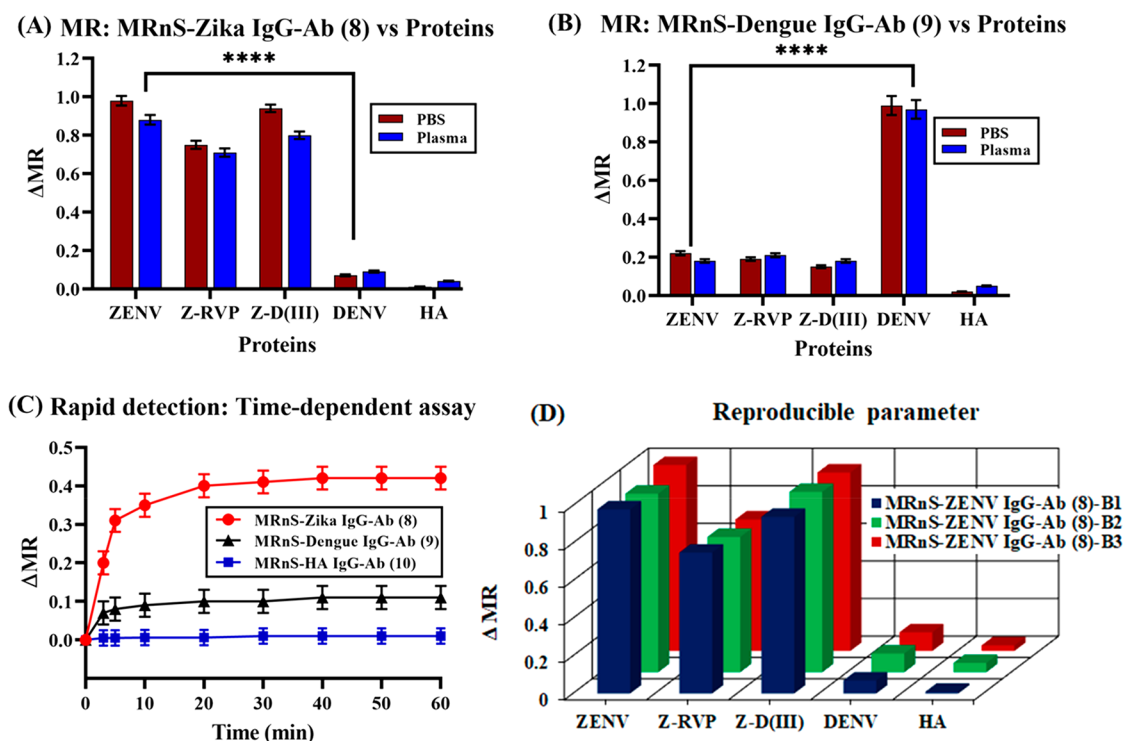


Figure 4. To further test the specificity of MRnS assay, (A) MRnS-Zika IgG-Ab and (B) MRnS-Dengue IgG-Ab ($[Fe] = 2.0$ mM) were incubated with Zika proteins, DENV and HA ($20 \mu\text{L}$, 120 nM) in PBS (brown) and plasma (blue) for 30 min at 25°C . (C) Time dependent assays were performed for the evaluation of rapid detection capability. ZENV (50 nM) was mixed separately with MRnS-Zika IgG-Ab (8), MRnS-Dengue IgG-Ab (9), and MRnS-HA IgG-Ab (10) and T2MR data points were collected for a time period of 60 min. Detectable T2MR changes were seen within 3 min of mixing. (D) Data represented for the batch-to-batch variability between MRnS preparations and for the reproducibility in the detection of ZIKV.

No significant change in ΔMR readout was observed with anti-Dengue IgG (ΔMR of 0.075). Control studies conducted with anti-HA IgG showed no binding further establishing the potential of MRnS for the assessment of molecular interactions with high specificity. For further cross-validation, surface plasmon resonance (SPR) studies were performed to analyze the interaction between ZENV/Z-D(III) and different antibodies (Figure 3B and D). Consistent with the MR data, anti-Zika-IgG binds to both ZENV and Z-D(III) with SPR response around 350 and $175 \mu\text{RIU}$, respectively. However, anti-Dengue-IgG showed substantial reduced binding with Z-D(III) and some binding with ZENV (30 and $75 \mu\text{RIU}$). In contrast, no measurable response was seen with anti-HA-IgG in both the cases (response $<10 \mu\text{RIU}$). Taken together, our MR and SPR results indicate that Z-D(III) can be used as a potential target for specific detection of Zika virus. Moreover, these results are in agreement with previous findings where Z-D(III) was shown to be a reliable target for diagnostic assays, and our functional MRnS platform can be used for this specific detection assay.

Rapid Detection of ZIKV and Analytical Sensitivity. As illustrated from our MR and SPR results (Figure 3), the extensive antigenic similarities between Zika and Dengue envelope proteins can compromise the diagnostic accuracy of serological tests achieved through the detection of antibodies. Recent studies⁴¹ have highlighted that the detection of Zika envelope protein/intact Zika virus can be a promising alternative to diagnose active infection with higher sensitivity and minimal cross-reactivity. To evaluate the potential application of our functional MRnS platform to detect intact

viruses, we conducted binding assays with MRnS-Zika IgG-Ab (8). We have selected Zika reporter virus (Z-RVP: antigenically similar to Zika virus) and Zika and Dengue proteins for this study. HA was also included as a negative control. For binding assays, a similar protocol was followed as noted above and as described in Materials and Methods. For T2MR testing with Zika, Dengue, and HA proteins, an optimal concentration of 120 nM was selected, and the test mixtures were incubated for 30 min at 25°C . The collected final ΔMR results are shown in Figure 4A. Among the selected proteins, ZENV, Z-RVP, and Z-D(III) showed strong binding (ΔMR values: 0.9 , 0.7 , and 0.9) with functional MRnS-Zika IgG-Ab. As expected, almost no change in ΔMR value was observed with negative control analyte (HA). It is important to note that only a nominal binding was observed with DENV. To further explore the extent of cross-reactivity, MRnS-Dengue IgG-Ab (9) was synthesized and similarly, the above proteins were tested using MR binding assay. As shown in Figure 4B, only DENV displayed strong binding. Some noticeable binding (comparable ΔMR values ~ 0.2) was observed for all the Zika proteins used, indicating higher level of cross-reactivity for anti-Dengue-IgG. Additionally, to replicate normal testing conditions, duplicate assays were also conducted in human plasma solutions. As presented in Figure 4A and B, ΔMR values in plasma solutions were in close agreement with that in PBS. These results further indicate higher analytical performance of MRnS assay without the need of extensive sample preparation.

With the successful binding results from multiple tests, we moved ahead with our experiments to assess the capability of functional MRnS for rapid detection. A concentration of 50

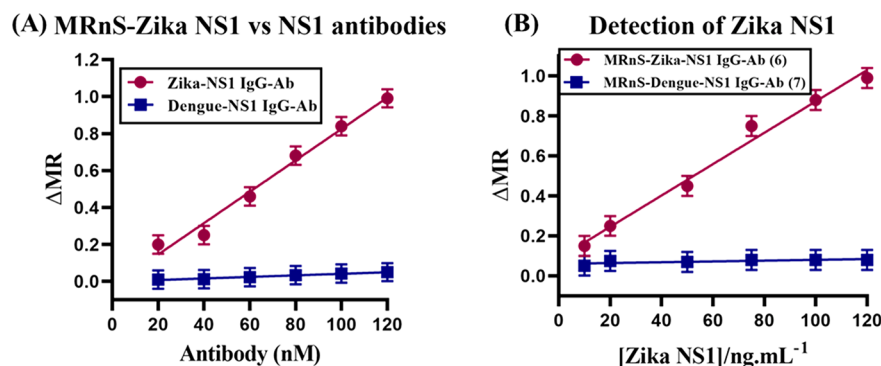


Figure 5. Functional MRnS assay for specific detection of Zika NS1. (A) Δ MR data showing linear correlation when increasing concentrations of Zika-NS1 IgG-Ab (10–120 nM) was incubated with MRnS-Zika-NS1 (S , $[\text{Fe}] = 2.0$ mM) for 30 min at 25 °C. MR data displaying lack of interaction between MRnS-Zika-NS1 ($[\text{Fe}] = 2.0$ mM) and Dengue-NS1 IgG-Ab (10–120 nM) demonstrates reliability of our formulated MRnS in Zika NS1 detection with minimal cross-reactivity with Dengue NS1. (B) MR experimental data obtained when MRnS-Zika-NS1 IgG-Ab (6) mixed with indicated concentrations of Zika NS1 (10–120 ng/mL) and further confirming for the minimum cross-reactivity with MRnS-Dengue-NS1 IgG-Ab (7).

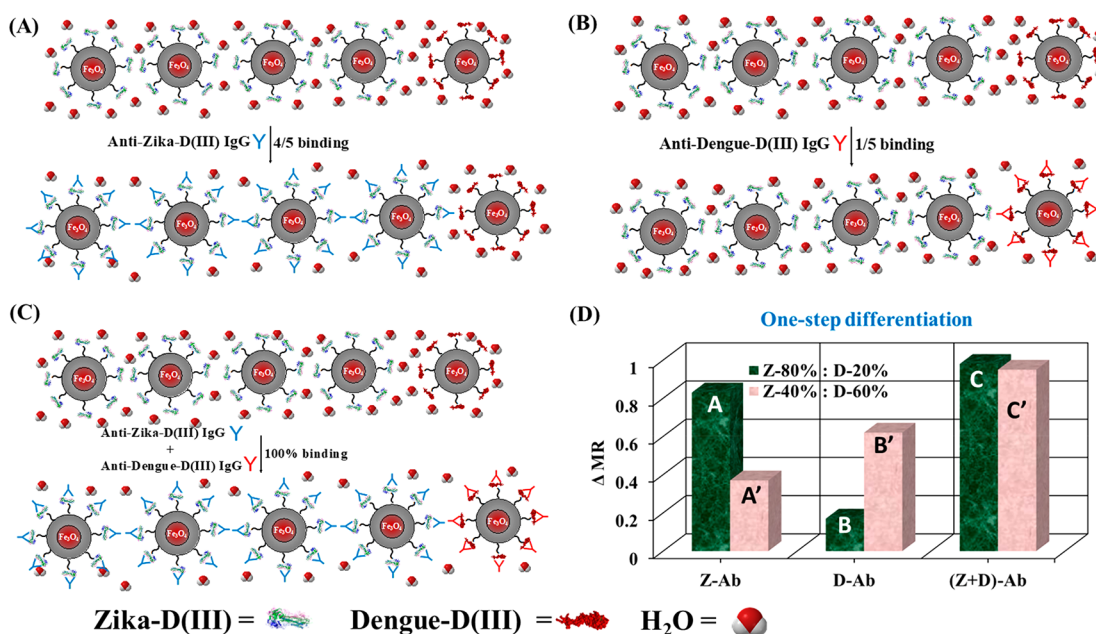


Figure 6. One step detection of Zika and Dengue using a mix solution of functional MRnS, 80% of MRnS-Zika-D(III) and 20% of MRnS-Dengue-D(III). (A) Schematic illustration of MR-based detection showing 80% binding if the sample contains only Zika antibody. (B) 20% binding expected if sample contains only Dengue antibody. (C) Co-infected sample expected to give 100% binding making our platform ideal for simultaneous detection of Zika and Dengue. (D) Experimental results obtained when 80 μ L of MRnS-Zika-D(III) and 20 μ L of MRnS-Dengue-D(III) ($[\text{Fe}] = 2.0$ mM) was mixed and incubated with anti-Zika-D(III) IgG (100 nM), anti-Dengue-D(III) IgG (100 nM), or a mixture of both the antibodies (100 nM each). (A'–C') Similar trend of results were recorded when 40 μ L of MRnS-Zika-D(III) and 20 μ L of MRnS-Dengue-D(III) ($[\text{Fe}] = 2.0$ mM) was mixed (D).

nM of ZENV was mixed separately with three different Abs-functional MRnS (8, 9, 10), each at $[\text{Fe}] = 2.0$ mM. To test for the specificity and sensitivity, we used Zika and Dengue antibody-conjugated MRnS, whereas functional MRnS-HA IgG-Ab (10) was included as a control. Incremental measurements were taken for a period of 60 min with detection of T2 changes observed within 3 min (Figure 4C). These results demonstrated that MRnS allows rapid and sensitive detection of ZIKV, therefore showcasing its promise to be implemented in clinical settings. In order to evaluate the batch-to-batch variability in our functional MRnS synthesis and to assess the reproducibility parameter in MRnS-based diagnostic assay, we have conducted tests with three independent preparations of MRnS-ZENV IgG-Ab (B1, B2, and B3). The detection

sensitivity tests were evaluated using samples of ZENV, Z-RVP, Z-D(III), DENV, and HA (each at 120 nM and spiked in 1X PBS). As determined by the collection of Δ MR values and shown in Figure 4D, the variability within the three-independent functional MRnS was found to be comparable. The intra-assay and interassay variability tests were conducted. For intra-assay variation, we selected samples corresponding to high, medium and low MR values. Each of these samples were measured in triplicate on the same day and the coefficient of variation (CV) was calculated (~ 2 –5%). To measure interassay variability, MR assays were conducted on the above samples using different batches of nanosensors. In addition, MR assays was performed on the same samples on

different days and the CV was found to be in the range of 2–12%.

Zika NS1: A Diagnostic Marker for Zika Detection.

Due to some extent of cross-reactivity seen between Zika and Dengue detection using the MRnS-Zika-D(III) (3) platform, we decided to further investigate to potentially improve specificity and assess sensitivity. Recent literature shows promising results with Z-NS1 seen to induce strong responses during ZIKV infection.⁴⁰ Easy customization of functional MRnS makes for testing interchangeable proteins and Abs feasible. With these factors in mind, we chose to study Z-NS1 in this context utilizing the aforementioned protocol. Experiments with MRnS-Zika NS1 (5) exhibited strongest binding with anti-Zika-NS1 IgG antibody (Figure 5A). Similarly, MRnS-Zika IgG-Ab (6) showed strongest binding with Zika NS1 (Figure 5B). As hypothesized, our MRnS-Zika NS1 (5) demonstrated high specificity for ZIKV even with Dengue NS1 present. Increasing concentrations of Zika-NS1 IgG-Ab and Dengue-NS1 IgG-Ab from 10–120 nM were added to fixed amounts of MRnS-Zika NS1 at $[Fe] = 2.0$ mM and as predicted, minimal cross-reactivity was observed (Figure 5A). The limit of detection also confirmed with the T2MR experiment (~ 10 ng/mL) showing sensitivity, indicating Zika NS1 shows promise as a reliable marker for ZIKV infection (Figure 5B).

Findings from each of these tests are particularly pertinent in light of previous infection or coinfection with DENV leading to false positives or ambiguous results. Our platform demonstrates both sensitivity and specificity in preliminary testing. This is significant due to tests results confounded with cross-reactivity in addition to patient's infected with ZIKV presenting with ambiguous or at times overlapping symptoms with DENV. Furthermore, our studies indicate rapid detection and consistent reproducibility demonstrating potential as accurate, rapid assays in areas with coexistence of both DENV and ZIKV.

One-Step Detection of ZIKV and DENV. We extrapolated the data from binding experiments and used our methods for the one-step detection of Zika and Dengue using a mixture of functional MRnS (Figure 6). Conjugating our nanosensors with Zika-D(III) and Dengue-D(III) proteins and mixed at 80% and 20%, respectively, would allow for more understanding of patient history of infection. As seen in Figure 6A, if only anti-Zika-D(III) IgG is present in the patient's sample, 80% binding would occur and could be confirmed through ΔMR . If DENV infection alone is present, 20% binding would occur (Figure 6B). If both Zika and Dengue antibodies are present in the sample, as in the case of coinfection, 100% binding would be observed (Figure 6C). We tested our simultaneous detection method with 80 μL of MRnS-Zika-D(III) and 20 μL of MRnS-Dengue-D(III) both at fixed concentration of $[Fe] = 2.0$ mM incubated with 100 nM of each antibody with predicted results observed in T2MR measurements, as shown in Figure 6D. Further experiments were performed to explore the effect of cross-infection in which Zika-D(III) and Dengue-D(III) functional MRnS were mixed at 40% and 60%, respectively, and expected results were collected (A'–C', Figure 6D). As diagnoses in cases of coinfection has proven challenging, this assay could prove important in patient care and management.

CONCLUSIONS

Considering the rapid spread of ZIKV infection, potential neurological disorders, and morbidity affecting all ages groups including fetal development resulting in congenital defects and death, the high likelihood of asymptomatic infections and known sexual transmission, accurate ZIKV testing is essential. Furthermore, there is an urgent need for testing that can distinguish between ZIKV and DENV due to cross-reactivity leading to ambiguous results and poor patient management. Challenged resources in areas where arboviruses are endemic further limit patient access to testing and rapid, accurate results. By designing a customizable MRnS platform, we were able to not only study ZIKV protein but also antibody response in the presence of corresponding DENV Abs and proteins. Our modality focused on proteins and Abs currently considered as strong candidates for ZIKV diagnostics leading to more specific therapeutic interventions. We found our novel MRnS could be successfully conjugated with both proteins and Abs to form a functional MRnS capable of detecting ZIKV infection despite coinfection with DENV. Additionally, this work confirms Zika-NS1 and Zika-D(III) as epitopes for further study for both sensitivity and specificity with Zika-NS1 showing higher specificity. This customizable library could be used to improve individualized medicine depending on region and infection serology in those areas. Additionally, we propose our simultaneous detection method for deeper understanding into patient history to improve intervention and therapeutic methods. Based on these findings, we propose our functional MRnS platform as a potential answer to the complex factors which have continued to limit assays in point-of-care settings. This platform could translate into a rapid, low-cost assay for ZIKV that additionally demonstrates high sensitivity and specificity even in the presence of DENV infection.

AUTHOR INFORMATION

Corresponding Author

Santimukul Santra – Department of Chemistry, Pittsburg State University, Pittsburg, Kansas 66762, United States of America; orcid.org/0000-0002-5047-5245; Phone: +1-620-235-4861; Email: ssantra@pittstate.edu

Authors

Tuhina Banerjee – Department of Chemistry, Pittsburg State University, Pittsburg, Kansas 66762, United States of America

Truptiben Patel – Department of Chemistry, Pittsburg State University, Pittsburg, Kansas 66762, United States of America

Oleksandra Pashchenko – Department of Chemistry, Pittsburg State University, Pittsburg, Kansas 66762, United States of America

Rebekah Elliott – Department of Chemistry, Pittsburg State University, Pittsburg, Kansas 66762, United States of America

Complete contact information is available at:
<https://pubs.acs.org/10.1021/acsabm.0c01264>

Funding

This research was supported by the National Institute of Health (NIH: 1 R03 AI132832-01) with funding to S.S. and T.B. and Kansas INBRE bridging grant (K-INBRE P20 GM103418) with funding to S.S.

Notes

The authors declare no competing financial interest.

ACKNOWLEDGMENTS

The authors would like to thank Dr. Sharon Willis from Integral Molecular for the kind gift of Zika Reporter Virus Particles (Z-RVP) for this study. We thank Ms. Lisa Whitworth and Oklahoma State University at Stillwater for providing TEM facility.

REFERENCES

- (1) Duffy, M. R.; Chen, T.-H.; Hancock, W. T.; Powers, A. M.; Kool, J. L.; Lanciotti, R. S.; Pretrick, M.; Marfel, M.; Holzbauer, S.; Dubray, C.; Guillaumot, L.; Griggs, A.; Bel, M.; Lambert, A. J.; Laven, J.; Kosoy, O.; Panella, A.; Biggerstaff, B. J.; Fischer, M.; Hayes, E. B. Zika virus outbreak on Yap Island, Federated States of Micronesia. *N. Engl. J. Med.* **2009**, *360*, 2536–2543.
- (2) Faria, N. R.; Azevedo, R. d. S. d. S.; Kraemer, M. U. G.; Souza, R.; Cunha, M. S.; Hill, S. C.; Theze, J.; Bonsall, M. B.; Bowden, T. A.; Rissanen, I.; Rocco, I. M.; Nogueira, J. S.; Maeda, A. Y.; Vasami, F. G. d. S.; Macedo, F. L. d. L.; Suzuki, A.; Rodrigues, S. G.; Cruz, A. C. R.; Nunes, B. T.; Medeiros, D. B. d. A.; Rodrigues, D. S. G.; Nunes Queiroz, A. L.; Silva, E. V. P. d.; Henriques, D. F.; Travassos da Rosa, E. S.; de Oliveira, C. S.; Martins, L. C.; Vasconcelos, H. B.; Casseb, L. M. N.; Smith, D. d. B.; Messina, J. P.; Abade, L.; Lourenco, J.; Alcantara, L. C. J.; Lima, M. M. d.; Giovanetti, M.; Hay, S. I.; de Oliveira, R. S.; Lemos, P. d. S.; Oliveira, L. F. d.; de Lima, C. P. S.; da Silva, S. P.; Vasconcelos, J. M. d.; Franco, L.; Cardoso, J. F.; Vianez-Junior, J. L. d. S. G.; Mir, D.; Bello, G.; Delatorre, E.; Khan, K.; Creatore, M.; Coelho, G. E.; de Oliveira, W. K.; Tesh, R.; Pybus, O. G.; Nunes, M. R. T.; Vasconcelos, P. F. C. Zika virus in the Americas: Early epidemiological and genetic findings. *Science* **2016**, *352*, 345–349.
- (3) 15 December 2016: Zika - Epidemiological Update. PAHO/WHO Pan American Health Organization. <https://www.paho.org/en/documents/15-december-2016-zika-epidemiological-update>.
- (4) WHO Situation Report. <http://apps.who.int/iris/bitstream/10665/254714/1/zikasitrep10Mar17-eng.pdf?ua=1>.
- (5) Sakkas, H.; Economou, V.; Papadopoulou, C. Zika virus infection: Past and present of another emerging vector-borne disease. *J. Vector Borne Disease* **2016**, *53*, 305–311.
- (6) Ventura, C. V.; Maia, M.; Bravo-Filho, V.; Góis, A. L.; Belfort, R., Jr. Zika virus in Brazil and macular atrophy in a child with microcephaly. *Lancet* **2016**, *387*, 228.
- (7) Brasil, P.; Pereira, J. P.; Moreira, M. E.; Ribeiro Nogueira, R. M.; Damasceno, L.; Wakimoto, M.; Rabello, R. S.; Valderramos, S. G.; Halai, U.-A.; Salles, T. S.; Zin, A. A.; Horovitz, D.; Daltro, P.; Boechat, M.; Raja Gabaglia, C.; Carvalho de Sequeira, P.; Pilotto, J. H.; Medialdea-Carrera, R.; Cotrim da Cunha, D.; Abreu de Carvalho, L. M.; Pone, M.; Machado Siqueira, A.; Calvet, G. A.; Rodrigues Baiao, A. E.; Neves, E. S.; Nassar de Carvalho, P. R.; Hasue, R. H.; Marschik, P. B.; Einspieler, C.; Janzen, C.; Cherry, J. D.; Bispo de Filippis, A. M.; Nielsen-Saines, K. Zika Virus Infection in Pregnant Women in Rio de Janeiro. *N. Engl. J. Med.* **2016**, *375*, 2321–2334.
- (8) van der Linden, V.; Filho, E. L. R.; Lins, O. G.; van der Linden, A.; Aragao, M. d. F. V. V.; Brainer-Lima, A. M.; Cruz, D. D. C. S.; Rocha, M. A. W.; Sobral da Silva, P. F.; Carvalho, M. D. C. G.; do Amaral, F. J.; Gomes, J. A.; Ribeiro de Medeiros, I. C.; Ventura, C. V.; Ramos, R. C. Congenital Zika syndrome with arthrogryposis: retrospective case series study. *BMJ* **2016**, *354*, i3899.
- (9) van der Linden, V.; Pessoa, A.; Dobyns, W.; Barkovich, A. J.; Junior, H. v. d. L.; Filho, E. L. R.; Ribeiro, E. M.; Leal, M. d. C.; Coimbra, P. P. d. A.; Aragao, M. d. F. V. V.; Vercosa, I.; Ventura, C.; Ramos, R. C.; Cruz, D. D. C. S.; Cordeiro, M. T.; Mota, V. M. R.; Dott, M.; Hillard, C.; Moore, C. A. Description of 13 Infants Born During October 2015–January 2016 With Congenital Zika Virus Infection Without Microcephaly at Birth - Brazil. *MMWR Morb Mortal Wkly Rep.* **2016**, *65*, 1343–1348.
- (10) Ventura, C. V.; Maia, M.; Dias, N.; Ventura, L. O.; Belfort, R. Zika: neurological and ocular findings in infant without microcephaly. *Lancet* **2016**, *387*, 2502.
- (11) Lindsey, N. P.; Staples, J. E.; Powell, K.; Rabe, I. B.; Fischer, M.; Powers, A. M.; Kosoy, O. L.; Mossel, E. C.; Munoz-Jordan, J. L.; Beltran, M.; Hancock, W. T.; Toews, K. E.; Ellis, E. M.; Ellis, B. R.; Panella, A. J.; Basile, A. J.; Calvert, A. E.; Laven, J.; Goodman, C. H.; Gould, C. V.; Martin, S. W.; Thomas, J. D.; Villanueva, J.; Mataia, M. L.; Sculli, R.; Gose, R.; Whelen, A. C.; Hills, S. L. Ability to Serologically Confirm Recent Zika Virus Infection in Areas with Varying Past Incidence of Dengue Virus Infection in the United States and U.S. Territories in 2016. *J. Clin. Microbiol.* **2018**, *56*, e01115–e01117.
- (12) Drain, P. K.; Hyle, E. P.; Noubary, F.; Freedberg, K. A.; Wilson, D.; Bishai, W. R.; Rodriguez, W.; Bassett, I. V. Diagnostic point-of-care tests in resource-limited settings. *Lancet Infect. Dis.* **2014**, *14*, 239–249.
- (13) Pashchenko, O.; Shelby, T.; Banerjee, T.; Santra, S. A comparison of optical, electrochemical, magnetic, and colorimetric point-of-care biosensors for infectious disease diagnosis. *ACS Infect. Dis.* **2018**, *4*, 1162–1178.
- (14) World Health Organization (WHO). Dengue and severe dengue. <https://www.who.int/news-room/fact-sheets/detail/dengue-and-severe-dengue>.
- (15) Bhatt, S.; Gething, P. W.; Brady, O. J.; Messina, J. P.; Farlow, A. W.; Moyes, C. L.; Drake, J. M.; Brownstein, J. S.; Hoen, A. G.; Sankoh, O.; Myers, M. F.; George, D. B.; Jaenisch, T.; Wint, G. R. W.; Simmons, C. P.; Scott, T. W.; Farrar, J. J.; Hay, S. I. The global distribution and burden of dengue. *Nature* **2013**, *496*, 504–507.
- (16) Theel, E. S.; Hata, D. J. Diagnostic Testing for Zika Virus: a Postoutbreak Update. *J. Clin. Microbiol.* **2018**, *56*, e01972–e01972.
- (17) Griffin, I.; Martin, S. W.; Fischer, M.; Chambers, T. V.; Kosoy, O.; Falise, A.; Ponomareva, O.; Gillis, L. D.; Blackmore, C.; Jean, R. Zika Virus IgM Detection and Neutralizing Antibody Profiles 12–19 Months after Illness Onset. *Emerging Infect. Dis.* **2019**, *25*, 299–303.
- (18) Mendoza, E. J.; Makowski, K.; Barairo, N.; Holloway, K.; Dimitrova, K.; Sloan, A.; Vendramelli, R.; Ranadheera, C.; Safronetz, D.; Drebot, M. A.; Wood, H. Establishment of a comprehensive and high throughput serological algorithm for Zika virus diagnostic testing. *Diagn. Microbiol. Infect. Dis.* **2019**, *94*, 140–146.
- (19) Lanciotti, R. S.; Kosoy, O. L.; Laven, J. J.; Velez, J. O.; Lambert, A. J.; Johnson, A. J.; Stanfield, S. M.; Duffy, M. R. Genetic and serologic properties of Zika virus associated with an epidemic, Yap State, Micronesia, 2007. *Emerging Infect. Dis.* **2008**, *14*, 1232–1239.
- (20) Bingham, A. M.; Cone, M.; Mock, V.; Heberlein-Larson, L.; Stanek, D.; Blackmore, C.; Likos, A. Comparison of Test Results for Zika Virus RNA in Urine, Serum, and Saliva Specimens from Persons with Travel-Associated Zika Virus Disease — Florida, 2016. *MMWR Morbidity and Mortality Weekly Report* **2016**, *65*, 475–478.
- (21) Paz-Bailey, G.; Rosenberg, E. S.; Doyle, K.; Munoz-Jordan, J.; Santiago, G. A.; Klein, L.; Perez-Padilla, J.; Medina, F. A.; Waterman, S. H.; Adams, L. E.; Lozier, M. J.; Bertran-Pasarell, J.; Garcia Gubern, C.; Alvarado, L. I.; Sharp, T. M. Persistence of Zika Virus in Body Fluids - Final Report. *N. Engl. J. Med.* **2018**, *379*, 1234–1243.
- (22) Keasey, S. L.; Pugh, C. L.; Jensen, S. M. R.; Smith, J. L.; Hontz, R. D.; Durbin, A. P.; Dudley, D. M.; O'Connor, D. H.; Ulrich, R. G. Antibody Responses to Zika Virus Infections in Environments of Flavivirus Endemicity. *Clin. Vaccine Immunol.* **2017**, *24*, e00036–17.
- (23) Martin, D. A.; Muth, D. A.; Brown, T.; Johnson, A. J.; Karabatsos, N.; Roehrig, J. T. Standardization of Immunoglobulin M Capture Enzyme-Linked Immunosorbent Assays for Routine Diagnosis of Arboviral Infections. *J. Clin. Microbiol.* **2000**, *38*, 1823–1826.
- (24) Rabe, I. B.; Staples, J. E.; Villanueva, J.; Hummel, K. B.; Johnson, J. A.; Rose, L.; Hills, S.; Wasley, A.; Fischer, M.; Powers, A. M. Interim Guidance for Interpretation of Zika Virus Antibody Test Results. *MMWR Morbidity and Mortality Weekly Report* **2016**, *65*, 543–546.

(25) Kikuti, M.; Tauro, L. B.; Moreira, P. S. S.; Campos, G. S.; Paploski, I. A. D.; Weaver, S. C.; Reis, M. G.; Kitron, U.; Ribeiro, G. S. Diagnostic performance of commercial IgM and IgG enzyme-linked immunoassays (ELISAs) for diagnosis of Zika virus infection. *Viol. J.* **2018**, *15*, 108.

(26) Koishi, A. C.; Suzukawa, A. A.; Zanluca, C.; Camacho, D. E.; Comach, G.; Duarte dos Santos, C. N. Development and evaluation of a novel high-throughput image-based fluorescent neutralization test for detection of Zika virus infection. *PLoS Neglected Trop. Dis.* **2018**, *12*, e0006342.

(27) Patterson, J.; Sammon, M.; Garg, M. Dengue, Zika and Chikungunya: Emerging Arboviruses in the New World. *West J. Emerg Med.* **2016**, *17*, 671–679.

(28) Izuan Abdul Rashid, J.; Azah Yusof, N. Laboratory Diagnosis and Potential Application of Nucleic Acid Biosensor Approach for Early Detection of Dengue Virus Infections. *Biosci., Biotechnol. Res. Asia* **2018**, *15*, 245–255.

(29) Durán, N.; Islan, G. A.; Durán, M.; Castro, G. R. Nanobiotechnology Solutions against *Aedes aegypti*. *J. Braz. Chem. Soc.* **2016**, *27*, 1139–1149.

(30) Benelli, G.; Caselli, A.; Canale, A. Nanoparticles for Mosquito Control: Challenges and Constraints. *J. King Saud Univ., Sci.* **2017**, *29*, 424–435.

(31) Nicolini, A. M.; McCracken, K. E.; Yoon, J.-Y. Future developments in biosensors for field-ready Zika virus diagnostics. *J. Biol. Eng.* **2017**, *11*, 7.

(32) Zhang, B.; Pinsky, B. A.; Ananta, J. S.; Zhao, S.; Arulkumar, S.; Wan, H.; Sahoo, M. K.; Abeynayake, J.; Waggoner, J. J.; Hopes, C.; Tang, M.; Dai, H. Diagnosis of Zika virus infection on a nanotechnology platform. *Nat. Med.* **2017**, *23*, 548–550.

(33) Yen, C.-W.; de Puig, H.; Tam, J. O.; Gómez-Márquez, J.; Bosch, I.; Hamad-Schifferli, K.; Gehrke, L. Multicolored Silver Nanoparticles for Multiplexed Disease Diagnostics: Distinguishing Dengue, Yellow Fever, and Ebola Viruses. *Lab Chip* **2015**, *15*, 1638–1641.

(34) Nawaz, M. H.; Hayat, A.; Catanante, G.; Latif, U.; Marty, J. L. Development of a portable and disposable NS1 based electrochemical immunosensor for early diagnosis of dengue virus. *Anal. Chim. Acta* **2018**, *1026*, 1–7.

(35) Omar, N. A. S.; Fen, Y. W.; Abdullah, J.; Chik, C. E. N. C. E.; Mahdi, M. A. Development of an optical sensor based on surface plasmon resonance phenomenon for diagnosis of dengue virus E-Protein. *Sensing and Bio-Sensing Research* **2018**, *20*, 16–21.

(36) Campos, E. V. R.; de Oliveira, J. L.; Abrantes, D. C.; Rogério, C. B.; Bueno, C.; Miranda, V. R.; Monteiro, R. A.; Fraceto, L. F. Recent Developments in Nanotechnology for Detection and Control of *Aedes aegypti*-Borne Diseases. *Front. Bioeng. Biotechnol.* **2020**, *8*, 102.

(37) Shelby, T.; Banerjee, T.; Zegar, I.; Santra, S. Highly Sensitive, Engineered Magnetic Nanosensors to Inverstigate the Ambiguous Activity of Zika Virus and Binding Receptors. *Sci. Rep.* **2017**, *7*, 7377.

(38) Banerjee, T.; Sulthana, S.; Shelby, T.; Heckert, B.; Jewell, J.; Woody, K.; Karimnia, V.; McAfee, J.; Santra, S. Multiparametric Magneto-fluorescent Nanosensors for the Ultrasensitive Detection of *E. coli* O157:H7. *ACS Infect. Dis.* **2016**, *2*, 667–673.

(39) Shelby, T.; Banerjee, T.; Kallu, J.; Sulthana, S.; Zegar, I.; Santra, S. Novel magnetic relaxation nanosensors: an unparalleled "spin" on influenza diagnosis. *Nanoscale* **2016**, *8*, 19605–19613.

(40) Santra, S.; Kaittanis, C.; Grimm, J.; Perez, J. M. Drug/dye-loaded, multifunctional iron oxide nanoparticles for combined targeted cancer therapy and dual optical/magnetic resonance imaging. *Small* **2009**, *5*, 1862–8.

(41) Draz, M. S.; Venkataramani, M.; Lakshminarayanan, H.; Saygili, E.; Moazeni, M.; Vasan, A.; Li, Y.; Sun, X.; Hua, S.; Yu, X. G.; Shafiee, H. Nanoparticle-enhanced electrical detection of Zika virus on paper microchips. *Nanoscale* **2018**, *10*, 11841–1184.